
MCTS-EP: Empowering Embodied Planning with Online Preference Optimization

Hang Xu^{*1,2} Zang Yu^{*2} Yehui Tang⁺² Pengbo Hu² Yuhao Tang^{‡3} Hao Dong^{4,5}

Abstract

This paper introduces MCTS-EP, an online learning framework that combines large language models (LLM) with Monte Carlo Tree Search (MCTS) for training embodied agents. MCTS-EP integrates three key components: MCTS-guided exploration for preference data collection, efficient multi-modal reasoning mechanism, and iterative training pipeline based on preference optimization. We theoretically prove that MCTS-EP achieves better performance bounds than conventional on-policy algorithms when the loss function is strongly convex, and demonstrate that it can be formulated as a search-enhanced variant of GAIL. MCTS-EP achieves state-of-the-art performance across several benchmarks. In ALFWorld, it achieves 92% and 87% success rates for textual and visual tasks. In WebShop, it reaches an average reward of 0.81. MCTS-EP also reduces average interaction steps from 18.7/19.5 to 10.2/9.9 steps in textual/visual ALFWorld.¹

1. Introduction

Recently, large language models (LLM) trained on internet-scale data have demonstrated strong capabilities in common-sense reasoning (Touvron et al., 2023; Bai et al., 2023; Team et al., 2024; Wei et al., 2022). Furthermore, vision-language models (VLM) effectively bridge the gap between language instructions and visual observations, enabling more robust multi-modal reasoning (Wang et al., 2024b; Li et al., 2023; Liu et al., 2024; Zhu et al., 2023). Building on these advancements, embodied agents can now perform complex decision-making tasks in interactive environments based on general commonsense knowledge (Wu et al., 2023a; Li et al., 2024; Stella et al., 2023).

A key challenge for decision-making tasks is that agents must reason over multi-modal information and sequentially decompose tasks into actionable steps (Jansen, 2020; Huang et al., 2022; Li et al., 2022). In the domain of text generation,

the state space of token is exponentially larger (Guo et al., 2025). Employing Monte Carlo Tree Search (MCTS) faces substantial computational cost. However, embodied agent’s action space is discrete and small when receive environment feedback. This making MCTS suitable for exploration in environments. Recent works have explored using MCTS (Coulom, 2006; Kocsis & Szepesvári, 2006) to enhance LLM reasoning (Zelikman et al., 2024; Zhao et al., 2024; Zhang et al., 2024). But these methods are not exclusively focused on embodied scenarios.

Several approaches have emerged to enhance embodied agents through feedback, preference optimization, and cross-modal learning. Reflexion (Shinn et al., 2024) uses linguistic feedback and episodic memory to enable agents to learn from trial-and-error without expensive model fine-tuning. IPR (Xiong et al., 2024) introduces step-level rewards and preference optimization to provide detailed supervision instead of outcome-based signals. SayCan (Ahn et al., 2022) uses visual navigation to collect information in the house to generate grounded plans. EMMA (Yang et al., 2024) takes a cross-modality approach by distilling LLM’s knowledge from text world to guide visual world learning.

Despite advances in embodied planning algorithms, several limitations remain. First, generating high-quality data is a persistent challenge. Most methods rely on imitation learning (Hussein et al., 2017), which depends entirely on expert demonstrations. Imitation learning faces quadratic error accumulation challenge in long-horizon tasks (Ross & Bagnell, 2010). Besides, these approaches lack sufficient exploration of interactive environments and fail to leverage knowledges from trial-and-error (Song et al., 2024). Second, many existing works focus on TextWorld (Côté et al., 2019), where agents depend on structured textual feedback and predefined candidate actions to guide planning. However, visual agents must infer actions and environmental feedback directly from camera inputs in real-world scenarios. EMMA (Yang et al., 2024) partially addresses this limitation through a multi-modal approach but struggles with repeated trial-and-error attempts, which are impractical in real-world applications. Lastly, methods like IPR leverage direct preference optimization (DPO) (Rafailov et al., 2024) for preference learning. But they rely on static

¹Code available at: <https://github.com/xuhang-2/Embodied-Agent-Planning>

datasets or random sampling to collect preference pairs, limiting the model to passively learn from predefined trajectories (Xiong et al., 2024). This results in offline trainings which can fail with high probability (Xie et al., 2024). In contrast, an online framework enables iterative learning through self-exploration, enhancing planning capabilities and generalization.

To address these limitations, we propose a multi-modal framework (MCTS-EP) that generates preference data and trains LLM for embodied agents online. MCTS-EP includes three components: 1) Preference Data Collection based on MCTS: We employ iteratively training LLM as policy model to guide MCTS to generate preference action pairs and success trajectories. We make a series of improvements to MCTS to improve the efficiency of data collection, 2) Selective State Representation for Multi-Modal Reasoning: We propose a new multi-modal planning pipeline that balances reasoning speed with memory utilization. 3) MCTS-Enhanced DPO: We design an MCTS-Enhanced DPO framework that combines expert fine-tuning, preference data collection, and iterative optimization to improve model’s planning capabilities.

The main contributions of this work can be summarized as:

1. Preference Data Collection based on MCTS: We propose an efficient and robust preference data collection method for embodied agent. In the process, MCTS can be seen as an implicit reward model.
2. MCTS-Enhanced DPO: We design a pipeline that maintains inference efficiency while incorporating memory during reasoning. The training process approximates offline DPO as multi-round online training, improving model performance in both accuracy and task efficiency.
3. We evaluate MCTS-EP on the ALFWorld and WebShop (Shridhar et al., 2020b; Yao et al., 2022a). Experimental results show that MCTS-EP achieves state-of-the-art performance in both score, success rate and task efficiency.

2. Related Work

Long-horizon Reasoning with Language Models. Recent LLMs have significantly advanced long-horizon reasoning (Touvron et al., 2023; Bai et al., 2023). Chain-of-thought prompting (Wei et al., 2022) enables step-by-step task decomposition. Several works combine MCTS with LLM for systematic exploration (Zelikman et al., 2024; Zhao et al., 2024; Zhang et al., 2024), while (Jiao et al., 2024) proposes a planning-based framework that synthesizes process rewards from offline trajectories to enhance reasoning without costly human annotations. Reflexion (Shinn et al., 2024)

uses feedback and memory for iterative improvement. However, these methods primarily target language-only tasks. VLM (Wang et al., 2024b; Li et al., 2023) bridge visual and linguistic understanding, enabling multi-modal reasoning (Chen et al., 2024a;b).

Task Planning for Embodied Agents. Task planning for embodied agents requires decomposing high-level goals into executable action sequences while considering environmental constraints. Traditional approaches rely heavily on structured action spaces and expert demonstrations (Hussein et al., 2017), limiting their applicability in dynamic environments. Recent works like SayCan (Ahn et al., 2022) have made progress incorporating visual grounding for more robust planning, while IPR (Xiong et al., 2024) introduces preference optimization to provide fine-grained supervision. EEMA (Yang et al., 2024) takes a cross-modal approach to transfer knowledge from text to visual domains, though it often requires multiple attempts to complete tasks successfully. APRICOT (Wang et al., 2024a) further advances this line of work by integrating active preference learning with constraint-aware planning, enabling robots to infer user preferences from sparse demonstrations while ensuring feasibility in real-world environments.

3. Method

3.1. Preliminary

In this section, we introduce the basic settings of MCTS-EP. Embodied task planning can be formulated as a partially observable Markov decision process (POMDP), defined by a tuple $\langle \mathcal{U}, \mathcal{A}, \mathcal{O}, \mathcal{S}, \mathcal{T}, \mathcal{R} \rangle$. \mathcal{U} is instruction space. \mathcal{A} is action space. \mathcal{O} is observation space. \mathcal{S} is state space. $s_t \in \mathcal{S}$ can be written as:

$$s_t = (u, a_1, o_1, \dots, a_t, o_t), \quad (1)$$

where $u_t \in \mathcal{U}$ is a natural language instruction, an example is "put a clean pan in countertop", $a_t \in \mathcal{A}$ is action in step t, $o_t \in \mathcal{O}$ is observation in step t, which can be either textual or visual.

$\mathcal{T} : \mathcal{S} \times \mathcal{A} \times \mathcal{S} \rightarrow [0, 1]$ is the transition function. $\mathcal{R} : \mathcal{S} \rightarrow [0, 1]$ is the reward function. In this paper, we use outcome reward function, only applying to terminal states. We define initial policy model π_{θ_0} and iterative policy model π_{θ_i} as LLM or VLM. The objective function is

$$\min_{\theta_i} \mathbb{E}_{s_t \sim \mathcal{S}} [D_{KL}(\pi_{\theta_i}(a_t^* | s_t) || \pi^*(a_t^* | s_t))], \quad (2)$$

where $\pi_{\theta_i}(a_t^* | s_t)$ is the predicted action distribution, $\pi^*(a_t^* | s_t)$ is the optimal policy distribution, a_t^* is the ground truth action.

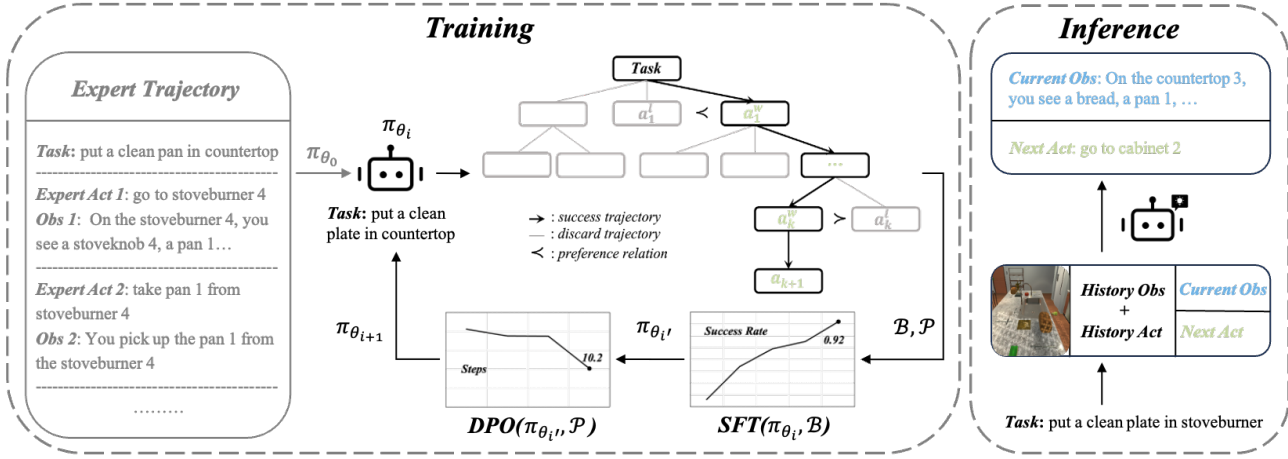


Figure 1. **Overview framework.** The framework consists of three key components: (1) MCTS-guided preference data collection, (2) selective state representation for multi-modal reasoning, and (3) iterative training pipeline.

3.2. Preference Data Collection based on MCTS

To generate step-level preference data, we decompose the planning process into several phases in the React-style (Yao et al., 2022b). In every planning process, we sample candidate action from the distribution of π_{θ_i} . We employ MCTS to collect preference data, capturing long-term action consequences through value propagation.

3.2.1. SEARCH TREE CONSTRUCTION

Starting from initial state node s_0 , MCTS builds a search tree through iterative four phases search: selection, expansion, simulation, and backup.

Selection: Starting from the root node, the algorithm recursively selects child nodes until reaching a leaf node using Predictor + Upper Confidence bounds applied to Trees (PUCT) (Rosin, 2011):

$$a_t^* = \operatorname{argmax}_{a \in \mathcal{A}} \left[Q(s_t, a) + c_{\text{puct}} \pi_{\theta_i}(a|s_t) \sqrt{\frac{N(s_t)}{1 + N(s_t, a)}} \right],$$

where $Q(s_t, a)$ is estimated action value, $N(s_t)$ is visit count of state s_t , $N(s_t, a)$ is visit count of action a at state s_t , c_{puct} is coefficient, $\pi_{\theta}(\cdot|s_t)$ is action distribution given s_t .

Expansion: We introduce a self-critic (Zhang et al., 2024) to improve expansion efficiency. For each leaf node s_t during selection, we employ the critic LLMs π_{θ_c} to evaluate whether expansion is necessary:

$$\text{expand}(s_t) = \begin{cases} \text{true} & \text{if } \pi_{\theta_c}(s_t) > \tau \\ \text{false} & \text{otherwise,} \end{cases} \quad (3)$$

where τ is a threshold. If $\text{expand}(s_t)$, the algorithm pro-

ceeds with standard expansion by sampling actions from policy model $\pi_{\theta}(\cdot|s_t)$ and adding corresponding child nodes.

Simulation: We employ greedy search to guide simulation. This approach combines the reasoning of LLM with the exploration of MCTS. The simulation continues until either reaching a terminal state s_{terminal} or the maximum depth d_{max} . The reward function r_o evaluates the final state to provide a reward:

$$r_o(s_{\text{terminal}}) = \begin{cases} 1 & \text{if task completed} \\ 0.5 & \text{if task partially completed} \\ 0 & \text{if task not completed.} \end{cases} \quad (4)$$

Backup: After simulation, reward are propagated back through action path. For each node s_t in the backup path, we update its statistics as follows:

$$\begin{aligned} N(s_t) &\leftarrow N(s_t) + 1, \\ V(s_t) &\leftarrow V(s_t) + \gamma \cdot r(s_{t+1}), \\ Q(s_t, a_t) &\leftarrow Q(s_t, a_t) \\ &+ \frac{1}{N(s_t, a_t)} [V(s_{t+1}) - Q(s_t, a_t)], \end{aligned} \quad (5)$$

where $V(s_{t+1})$ is the simulated value from the child node, $r(s_{t+1})$ is discount reward propagated back through the simulation path with discount factor γ .

3.2.2. DATA COLLECTION FROM SEARCH TREE

We can extract two datasets from constructed search tree. **Success Trajectory Dataset \mathcal{B} :** For a single natural language task, multiple valid solution paths may exist. For instance, given the task "put a clean pan on the table", there

could be multiple pans in the environment. While an expert trajectory might demonstrate picking up a pan from the countertop, the agent could alternatively retrieve it from other valid containers.

We collect all successful paths discovered during Monte Carlo tree search into a success trajectory buffer $\mathcal{B} = \{(u, a_1, \dots, o_T)^i\}_{i=1}^N$, where N is the number of successful trajectories. These high-quality trajectories serve as online training data and can be used to fine-tune iterative policy network π_{θ_i} .

Preference Pairs Dataset \mathcal{P} : At any given state, multiple actions may lead to successful task completion. During MCTS’s backup, each node along the path receives updated reward estimates. We leverage this information to create preference pairs at branching nodes. Specifically, for each decision point s_t , we can generate ordered pairs (a_i, a_j) where actions are ranked according to their estimated action values

3.3. Selective State Representation for Multi-Modal Reasoning

In real-world applications, robots get observation from continuous camera feeds. At each timestep t , the agent receives a raw image observation o_t . Policy model π_{θ_i} processes o_t to predict next action a_t and extract key textual information τ_t (like object labels or spatial relationships):

$$a_t, \tau_t = \pi_{\theta}(s_t) \quad (6)$$

For long-horizon tasks, storing all historical observations for reasoning is computationally expensive. We optimize computational cost by storing only textual descriptions $\{\tau_1, \dots, \tau_{t-1}\}$ and actions from previous steps, while keeping the full image observation o_t only for current timestep. The state representation evolves as follows:

- Previous state: $s_{t-1} = (u, a_1, \tau_1, \dots, a_{t-1}, \tau_{t-1})$
- Current state: $s_t = s_{t-1} \cup \{a_t, o_t\}$

Visual-language models can thus operate efficiently while preserving critical environmental details.

3.4. MCTS-Enhanced DPO

MCTS-EP is designed to iteratively improve agent’s performance by MCTS for exploration and data generation. Starting from an initial policy model π_{θ_0} , the framework alternates between data generation and model updates. At iteration t , MCTS-EP performs following steps:

1. Data generation with MCTS (Section 3.2): Using current policy model π_{θ_i} , MCTS is applied to generate success trajectory data \mathcal{B} and preference pairs data \mathcal{P} .

2. Imitation learning on expert trajectories: The training process warms up by leveraging expert trajectories $\mathcal{D}_{\text{expert}}$ for pre-trained LLM/VLM to initialize policy model π_{θ_0} .
3. Fine-tuning on success trajectory data \mathcal{B} : Success trajectory data is used to fine-tune the policy model π_{θ_i} , incorporating successful attempt to enhance model performance through iterative updates.
4. Preference optimization on preference data \mathcal{P} : Preference pairs data \mathcal{P}_t is used to further fine-tune the model, aligning the policy with task-specific preferences.

3.4.1. IMITATION LEARNING WITH EXPERT TRAJECTORY

The first stage of the process involves Supervised Fine-Tuning (SFT) based on expert demonstrations $\mathcal{D}_{\text{expert}}$. In embodied scenarios, gathering large quantities of high-quality demonstrations is often costly and challenging. Therefore, small datasets serve to train the initial policy model π_{θ_0} to produce properly formatted, task-compliant outputs. The performance of policy model π_{θ_0} relies on following continuous improvement process.

Specifically, we denote expert trajectory $e_u \in \mathcal{D}_{\text{expert}}$ as $e_u = (u, a_1^*, a_2^*, \dots, a_k^*)$, where a_t^* is the best action at step t . Based on e_u , we can get expert terminal state $s_{u_t} = (u, a_1^*, o_1, \dots, a_k^*, o_k)$. Our object is to minimize loss function:

$$\begin{aligned} \mathcal{L}_{\text{SFT}}(\theta) &= -\mathbb{E}_{e_u \sim \mathcal{D}_{\text{expert}}} [\log \pi_{\theta}(e_u|u)] \\ &= -\mathbb{E}_{e_u \sim \mathcal{D}_{\text{expert}}} \left[\sum_k \log \pi_{\theta}(a_k|s_{u_{k-1}}) \right], \quad (7) \end{aligned}$$

where $s_{u_{k-1}} = (u, a_1^*, o_1, \dots, a_{k-1}^*, o_{k-1})$. SFT provide a good starting point for further optimization and exploration.

3.4.2. FINE-TUNING WITH SUCCESS TRAJECTORY DATA

After obtaining the initial policy model π_{θ_0} , MCTS leverages the initial policy π_{θ_0} to guide the search process and generate trajectories. We can get preference pairs dataset \mathcal{P} and success trajectory dataset \mathcal{B} . Each success trajectory in \mathcal{B} can be seen as a terminal state s_T when the trajectory satisfies task-specific objectives. s_T is composed of a sequence of observation-action pairs.

Formally, the objective is to minimize the negative log-likelihood:

$$\mathcal{L}_{\text{SFT}}(\theta) = -\mathbb{E}_{s_T \sim \mathcal{B}} \left[\sum_{t=1}^T \log \pi_{\theta}(a_t|s_{t-1}) \right]. \quad (8)$$

Compared to the initial imitation learning stage, fine-tuning with success trajectories enables the policy to adapt based on its own exploration of the environment. The use of MCTS allows for the discovery of trajectories that may not be present in the expert dataset $\mathcal{D}_{\text{expert}}$, enabling the policy to generalize beyond the constraints of the expert demonstrations. Besides, since the outcome reward model r_o directly evaluates whether a trajectory achieves the task objective, the fine-tuning process optimizes the policy with respect to task-specific goals rather than purely imitating expert behavior.

3.4.3. PREFERENCE OPTIMIZATION WITH PREFERENCE DATA

DPO improves the policy model’s commonsense understanding while enhancing task efficiency, such as reducing steps needed for object finding.

To achieve this alignment, preference data \mathcal{P} is utilized. Each preference in \mathcal{P} is represented as a tuple (a_t^w, a_t^l, s_{t-1}) , where a_t^w denotes the winning action that leads to a higher reward, a_t^l denotes the losing action with a lower reward. The preference data is used to construct a contrastive objective that encourages the policy to assign higher probabilities to a_t^w over a_t^l in the same context s_{t-1} . Formally, the DPO objective is defined as:

$$\mathcal{L}_{\text{DPO}}(\theta) = -\mathbb{E}_{(a_t^w, a_t^l, s_{t-1}) \sim \mathcal{P}} [\log(\sigma(\beta \cdot (\log(\frac{\pi_\theta(a_t^w | s_{t-1})}{\pi_{\text{ref}}(a_t^w | s_{t-1})}) - \log(\frac{\pi_\theta(a_t^l | s_{t-1})}{\pi_{\text{ref}}(a_t^l | s_{t-1})}))))], \quad (9)$$

where $\pi_\theta(a_t^w | s_{t-1})$ and $\pi_\theta(a_t^l | s_{t-1})$ are the conditional probabilities assigned by the policy π_θ to a_t^w and a_t^l , respectively.

The preference data \mathcal{P} is typically derived from policy model exploration or expert demonstrations. For a given state s_{t-1} , the model evaluates multiple candidate actions and their resulting outcomes. A preference is constructed whenever $Q(s_t, a_t^w) > Q(s_t, a_t^l)$, indicating that a_t^w leads to a more favorable outcome compared to a_t^l .

Complete MCTS-EP algorithm is summarized in Algorithm 1. The algorithm combines imitation learning, fine-tuning with success trajectories, and direct performance optimization to refine the policy model iteratively. MCTS-guided exploration enables the model to learn from successful experiences. Preference optimization helps the model understand and incorporate task-specific preferences. This integrated approach addresses the challenges of both exploration and optimization in complex embodied environments.

Algorithm 1 MCTS-Enhanced DPO

Input: Initial policy model π_{θ_0} , expert demonstrations $\mathcal{D}_{\text{expert}}$
Output: Optimized policy model π_θ
Phase 1: Imitation Learning
for $e_u = (u, a_1^*, \dots, a_k^*) \in \mathcal{D}_{\text{expert}}$ **do**
 $s_{u_{k-1}} \leftarrow (u, a_1^*, o_1, \dots, a_{k-1}^*, o_{k-1})$
 Minimize $\mathcal{L}_{\text{SFT}}(\theta) = -\sum_k \log \pi_\theta(a_k | s_{u_{k-1}})$
end for
Phase 2: Iterative Improvement
for iteration $i = 1$ to T **do**
 $\mathcal{B}, \mathcal{P} \leftarrow \text{MCTS}(\pi_{\theta_i})$ {Step 1: Generate success and preference data}
 for $s_T \in \mathcal{B}$ **do**
 Minimize $\mathcal{L}_{\text{SFT}}(\theta) = -\sum_{t=1}^T \log \pi_\theta(a_t | s_{t-1})$
 {Step 2: Fine-tune with Success Trajectories}
 end for
 for $(a_t^w, a_t^l, s_{t-1}) \in \mathcal{P}$ **do**
 $p_w \leftarrow \log(\pi_\theta(a_t^w | s_{t-1}) / \pi_{\text{ref}}(a_t^w | s_{t-1}))$
 $p_l \leftarrow \log(\pi_\theta(a_t^l | s_{t-1}) / \pi_{\text{ref}}(a_t^l | s_{t-1}))$
 Minimize $\mathcal{L}_{\text{DPO}}(\theta) = -\log(\sigma(\beta(p_w - p_l)))$ {Step 3: Direct Preference Optimization}
 end for
 $\theta_{i+1} \leftarrow \theta_i$ {Update model parameters}
end for
return π_θ

4. Theory Analysis

4.1. MCTS Performance Bounds

We provide theoretical performance guarantees for MCTS-based policies compared to conventional on-policy algorithms. Our analysis demonstrates that MCTS exhibits superior bounds under certain conditions.

Theorem 4.1. *Let π_θ be a policy represented by a language model and π_{mcts} be the policy derived from Monte Carlo Tree Search with Upper Confidence Bounds. For any state s , if the loss function l is strongly convex, then:*

$$\mathbb{E}[l(s, \pi_{\text{mcts}})] \leq \mathbb{E}[l(s, \pi_\theta)].$$

The complete proof of Theorem 4.1 is presented in Section A.1. Our proof follows a similar structure to DAgger (Ross et al., 2011), but extends it to the MCTS setting. This theoretical guarantee provides a formal foundation for the empirical success of MCTS in various decision-making scenarios and offers insights into why MCTS-enhanced policies tend to outperform standard policy networks.

4.2. MCTS-EP as Search-Enhanced GAIL Variant

Generative Adversarial Imitation Learning (GAIL) (Ho & Ermon, 2016) optimizes policies via adversarial training to

match the state-action occupancy measure of expert demonstrations. Traditional GAIL uses a discriminator to distinguish between expert and learned policy trajectories. In this section, we show that MCTS-EP can be viewed as a search-enhanced variant of GAIL, where the MCTS serves as an implicit discriminator through its value estimation process. This connection is formally established in the following theorem:

Theorem 4.2. *Let cost regularization is*

$$\psi(a) = c * \frac{\sqrt{\ln t}}{t * \rho_{\pi}(s, a)} + \mathbb{E}_{\pi_E} [\log \pi_E(a|s)],$$

MCTS-EP can be approximately formulated as GAIL framework.

The complete proof can be found in Section A.2. This formulation reveals a two-stage optimization process. The Lower Confidence Bound LCB (Rashidinejad et al., 2021) policy first generates a value function that serves as the cost function in IRL (Ng & Russell, 2000). DPO maximizes the log-probability difference between preferred and rejected actions through entropy-regularized optimization. This theoretical analysis leads to the following important corollary:

Corollary 4.3. *MCTS search process in MCTS-EP implicitly performs cost function learning, while the DPO optimization corresponds to policy improvement with respect to this learned cost function. This two-stage process ensures both explorations through MCTS and effective policy updates through DPO.*

5. Experiments

In this section, we conduct several experiments to validate the effectiveness of MCTS-EP. Our framework demonstrates better performance compared to baselines and SOTA methods.

5.1. Experiment Settings

Datasets We evaluate MCTS-EP on the ALFWorld (Shridhar et al., 2020b) and WebShop (Yao et al., 2022a) benchmark. ALFWorld extends the ALFRED (Shridhar et al., 2020a) dataset, using the AI2-THOR (Kolve et al., 2017) simulator to create a realistic household environment. It features a cross-modal framework for embodied household tasks, combining high-fidelity visual environments with text-based counterparts. WebShop is a web-based problem-solving benchmark that tests agents to navigate an e-commerce website to locate and purchase products given requests from clients

Training Setup We utilize Llama-3.1-8B-Instruct (Dubey et al., 2024) as the base model for verbal environments and Qwen2-VL-7B-Instruct (Wang et al., 2024b) for vision-based tasks. Llama-3.2-Vision-11B-Instruct was excluded

from our experiments due to issues with generating repetitive outputs and triggering warnings related to safety guideline violations. Detailed experimental settings and hyperparameters can be found in Section B.

Baselines To evaluate the effectiveness of our proposed method, we compare MCTS-EP against several baselines and state-of-the-art (SOTA) agents on the ALFWorld benchmark. The categorization and selection of baselines follow the methodology from EMMA (Yang et al., 2024). For textual environments, we evaluate three types of baselines: transformer-based models, such as BUTLER (Shridhar et al., 2020b) and GPT-BUTLER (Micheli & Fleuret, 2021); feedback-driven methods, including ReAct (Yao et al., 2022b), Reflexion (Shinn et al., 2024), and DEPS (Wang et al., 2023), which leverage reasoning traces, environmental feedback, or self-explanations to refine actions; and multi-agent collaboration approaches, such as AutoGen (Wu et al., 2023b), which enable coordination between multiple LLM agents to tackle complex tasks. For visual environments, we evaluate several baselines, including MiniGPT-4 (Zhu et al., 2023), BLIP-2 (Li et al., 2023), LLaMA-Adaptor (Gao et al., 2023), and InstructBLIP (Dai et al., 2023), which integrate visual and textual understanding through VLM, as well as EMMA (Yang et al., 2024), a multi-modal agent designed specifically for embodied tasks with enhanced cross-modal reasoning capabilities. We adopt the baseline training methods from IPR (Xiong et al., 2024), including PPO (Schulman et al., 2017), RFT (Yuan et al., 2023), and ETO (Song et al.), and additionally incorporate agent method like ReACT and Reflexion as WebShop baselines.

Evaluation Metrics We evaluate all methods using standard metrics across different benchmarks. For the ALFWorld benchmark, we measure both the success rate (percentage of successfully completed tasks) and the average number of interaction steps required per task completion, which reflects the agent’s decision-making efficiency. For the WebShop benchmark, following the evaluation protocol in IPR (Xiong et al., 2024), we report the average reward computed over 200 test episodes.

5.2. Experimental Results

Execution Time for MCTS-EP. While computational cost remains a primary concern for MCTS algorithms, our optimized implementation achieves practical efficiency. Using Llama-3.1-8B as the policy model with search parameters (max depth=10, width=3, simulations=3), our MCTS-EP completes each ALFWorld task in 4 minutes on dual A100 GPUs. This yields a full search tree containing 87 SFT trajectories and 28 preference pairs per episode.

MCTS-EP achieves SOTA in both visual and textual environments. We evaluate MCTS-EP against all base-

Table 1. ALFWorld Success Rate

TYPE	METHOD	SUCCESS RATE	PICK&PLACE	CLEAN&PLACE	HEAT&PLACE	COOL&PLACE	LOOK-IN-LIGHT	PICK-2&PLACE
TEXT	BUTLER	0.26	0.31	0.41	0.69	0.27	0.12	0.29
TEXT	GPT-BUTLER	0.69	0.62	0.81	0.85	0.78	0.50	0.47
TEXT	REACT	0.54	0.71	0.65	0.62	0.44	0.28	0.35
TEXT	REFLEXION	0.91	0.96	1.00	0.81	0.83	0.94	0.88
TEXT	DEPS	0.76	0.93	0.50	0.80	1.00	1.00	0.00
TEXT	AUTOGEN	0.77	0.92	0.74	0.78	0.86	0.83	0.41
TEXT	IPR	0.75	-	-	-	-	-	-
TEXT	MCTS-EP (OURS)	0.92	1.00	1.00	0.91	0.80	1.00	0.67
VISION	MINIGPT-4	0.16	0.04	0.00	0.19	0.17	0.67	0.06
VISION	BLIP-2	0.04	0.00	0.06	0.04	0.11	0.06	0.00
VISION	LLAMA-ADAPTER	0.13	0.17	0.10	0.27	0.22	0.00	0.00
VISION	INSTRUCTBLIP	0.22	0.50	0.26	0.23	0.06	0.17	0.00
VISION	EMMA	0.82	0.71	0.94	0.85	0.83	0.88	0.67
VISION	MCTS-EP (OURS)	0.87	0.90	1.00	0.82	0.80	1.00	0.50

Table 2. ALFWorld Steps Counts

TYPE	METHOD	STEPS	PICK&PLACE	CLEAN&PLACE	HEAT&PLACE	COOL&PLACE	LOOK-IN-LIGHT	PICK-2&PLACE
TEXT	GPT-BUTLER	18.8	18.4	18.4	12.7	15.6	24.4	26.6
TEXT	REACT	20.6	18.1	18.8	18.2	23.2	23.7	25.5
TEXT	REFLEXION	18.7	17.4	17.0	19.4	21.6	16.9	21.6
TEXT	MCTS-EP (OURS)	10.2	11.5	9.2	12.3	8.8	8.7	11.8
VISION	MINIGPT-4	26.9	29.0	30.0	26.3	26.7	17.7	28.9
VISION	BLIP-2	29.5	30.0	29.3	29.9	28.2	29.2	30.0
VISION	LLAMA-ADAPTER	27.5	26.4	28.6	24.2	26.7	30.0	30.0
VISION	INSTRUCTBLIP	26.2	21.5	25.0	27.2	28.9	26.8	30.0
VISION	EMMA	19.5	19.3	17.5	19.6	19.9	19.6	22.4
VISION	MCTS-EP (OURS)	9.9	6.8	10.2	13.1	10.9	6.4	15.3

Table 3. WebShop Average Reward

Type	Setting	WebShop
Training	Llama-2-7B + PPO	0.64
	Llama-2-7B + RFT	0.63
	Llama-3-8B + SFT	0.61
	Llama-3-8B + ETO	0.66
	Llama-3-8B + IPR	0.72
Agent	ReACT(Yao et al., 2022b)	0.66
	Reflexion (Shinn et al., 2024)	0.35
	ReACT(GPT-4o)	0.54
	ReACT(Claude 3.7)	0.43
Ours	MCTS-EP	0.81

lines in both textual and visual environments on the ALFWorld and WebShop. Results are summarized in Table 1, Table 2 and Table 3 with baseline results sourced from (Yang et al., 2024) and (Xiong et al., 2024). Our proposed method, MCTS-EP, demonstrates significant improvements over all baselines, achieving state-of-the-art performance in both environments.

Optimized Task Completion Rate. MCTS-EP outperforms all baselines in ALFWorld success rate, surpassing the previous textual SOTA Reflexion (91%) (Shinn et al., 2024) and visual SOTA EMMA (82%) (Yang et al., 2024). Notably, Reflexion and EMMA require multiple attempts to achieve their final results, whereas our method completes tasks in a single attempt. These performances gains can be primarily attributed to the online nature of MCTS-EP, which enables dynamic planning and decision-making during task execution. Online MCTS-EP is able to handle dynamic and partially observable environments effectively. This flexibility allows the agent to generalize its strategies and maintain high success rates across diverse tasks, regardless of their complexity or dependencies.

Fewer Steps, Better Task Performance. MCTS-EP re-

Table 4. ALFWorld Ablation Study Result

METHOD	SUCCESS RATE	PICK&PLACE	CLEAN&PLACE	HEAT&PLACE	COOL&PLACE	LOOK-IN-LIGHT	PICK-2&PLACE
w/o FINE-TUNING (\mathcal{B})	0.53 (8.7)	0.60 (4.8)	0.57 (9.5)	0.36 (14.0)	0.80 (9.9)	0.56 (6.0)	0.17 (9.0)
w/o DPO	0.87 (11.8)	0.90 (10.3)	0.93 (9.8)	0.91 (16.9)	0.80 (11.4)	1.00 (9.1)	0.50 (16.7)
MCTS-EP (OURS)	0.87 (9.9)	0.90 (6.8)	1.00 (10.2)	0.82 (13.1)	0.80 (10.9)	1.00 (6.4)	0.50 (15.3)

Table 5. WebShop Ablation Study Result

Method	Average Reward
w/o Fine-Tuning (\mathcal{B})	0.61
w/o DPO	0.68
MCTS-EP (Ours)	0.81

duces the interaction steps to 10.22 in text and 9.9 in vision ALFWorld, a significant improvement compared to Reflexion’s 18 and EMMA’s 19.5. The performance gains are primarily attributed to DPO, allowing the embodied agent to refine its commonsense understanding of the environment. This ensures that the agent focuses on the most relevant actions to achieve task objectives, avoiding unnecessary exploration. These results also emphasize the model’s capability to integrate cross-modal reasoning seamlessly. By leveraging its multi-modal understanding, MCTS-EP achieves greater efficiency in environments requiring both textual and visual inputs.

Optimization in High-Dimensional Action Space. MCTS-EP also achieves SOTA performance on the Webshop benchmark, which has a high-dimensional action space. While standard MCTS struggles with large action spaces, and Reflexion (Shinn et al., 2024) admits difficulty in tasks requiring extensive exploration, our method overcomes these limitations. By iteratively guiding the policy, we dynamically prune low-value actions—suppressing their probabilities—to focus exploration efficiently, achieving a final average reward of 0.81.

5.3. Ablation Study

To evaluate the impact of individual components in our framework, we conducted ablation experiments on the two key steps of MCTS-EP: Fine-tuning with success trajectory data and DPO. The results are presented in Table 4 and Table 5. In our table, “w/o Fine-Tuning (\mathcal{B})” represents that we omit the MCTS exploration phase and fine-tune the model solely using expert trajectory data. “w/o DPO” indicates that we remove DPO training with preference pairs obtained from MCTS exploration, while retaining the fine-tuning process with successful trajectories discovered through MCTS. MCTS-EP is complete method.

Online Fine-tuning Enhances Accuracy. Removing the fine-tuning step with success trajectory results in a signifi-

cant drop in performance, with the success rate decreasing from 87% to 53%. This demonstrates the critical role of fine-tuning success trajectory data in improving the model’s ability to adapt to task-specific requirements and align its outputs with desired goals.

DPO Improves Commonsense. When DPO is removed, the success rate remains at 87%, the same as the full framework. However, the average interaction steps increase significantly, from 9.9 to 11.8, indicating a loss in decision-making efficiency. This highlights how DPO helps refine the model’s commonsense reasoning and action prioritization, enabling the agent to make more efficient decisions during task execution.

6. Conclusion

This paper presents MCTS-EP, an online framework for training embodied agents that combines MCTS with DPO. Our approach addresses key challenges in embodied environments based on three components: (1) an efficient preference data collection method, (2) a selective state representation strategy for multi-modal reasoning, and (3) an online framework that iteratively improves model performance.

We provide theoretical analysis for our framework, proving that MCTS-based policies achieve better performance bounds. MCTS-EP demonstrates SOTA performance in both textual and visual environments. Ablation studies highlight the roles of the framework’s components: fine-tuning with success trajectories enhances task completion accuracy, while DPO significantly improves the model’s commonsense reasoning. These results suggest that combining MCTS-guided exploration with preference optimization creates a robust foundation for training embodied agents.

References

- Aeronautiques, C., Howe, A., Knoblock, C., McDermott, I. D., Ram, A., Veloso, M., Weld, D., Sri, D. W., Barrett, A., Christianson, D., et al. Pddl—the planning domain definition language. *Technical Report, Tech. Rep.*, 1998.
- Ahn, M., Brohan, A., Brown, N., Chebotar, Y., Cortes, O., David, B., Finn, C., Fu, C., Gopalakrishnan, K., Hausman, K., et al. Do as i can, not as i say: Grounding language in robotic affordances. *arXiv preprint arXiv:2204.01691*,

- 2022.
- Auer, P. Finite-time analysis of the multiarmed bandit problem, 2002.
- Bai, J., Bai, S., Chu, Y., Cui, Z., Dang, K., Deng, X., Fan, Y., Ge, W., Han, Y., Huang, F., et al. Qwen technical report. *arXiv preprint arXiv:2309.16609*, 2023.
- Chen, B., Xu, Z., Kirmani, S., Ichter, B., Sadigh, D., Guibas, L., and Xia, F. Spatialvlm: Endowing vision-language models with spatial reasoning capabilities. In *Proceedings of the IEEE/CVF Conference on Computer Vision and Pattern Recognition*, pp. 14455–14465, 2024a.
- Chen, L., Li, B., Shen, S., Yang, J., Li, C., Keutzer, K., Darrell, T., and Liu, Z. Large language models are visual reasoning coordinators. *Advances in Neural Information Processing Systems*, 36, 2024b.
- Côté, M.-A., Kádár, A., Yuan, X., Kybartas, B., Barnes, T., Fine, E., Moore, J., Hausknecht, M., El Asri, L., Adada, M., et al. Textworld: A learning environment for text-based games. In *Computer Games: 7th Workshop, CGW 2018, Held in Conjunction with the 27th International Conference on Artificial Intelligence, IJCAI 2018, Stockholm, Sweden, July 13, 2018, Revised Selected Papers 7*, pp. 41–75. Springer, 2019.
- Coulom, R. Efficient selectivity and backup operators in monte-carlo tree search. In *International conference on computers and games*, pp. 72–83. Springer, 2006.
- Dai, W., Li, J., Li, D., Tiong, A., Zhao, J., Wang, W., Li, B., Fung, P., and Hoi, S. InstructBLIP: Towards general-purpose vision-language models with instruction tuning. In *Thirty-seventh Conference on Neural Information Processing Systems*, 2023. URL <https://openreview.net/forum?id=vvoWPYqZJA>.
- Dubey, A., Jauhri, A., Pandey, A., Kadian, A., Al-Dahle, A., Letman, A., Mathur, A., Schelten, A., Yang, A., Fan, A., et al. The llama 3 herd of models. *arXiv preprint arXiv:2407.21783*, 2024.
- Gao, P., Han, J., Zhang, R., Lin, Z., Geng, S., Zhou, A., Zhang, W., Lu, P., He, C., Yue, X., et al. Llama-adapter v2: Parameter-efficient visual instruction model. *arXiv preprint arXiv:2304.15010*, 2023.
- Guo, D., Yang, D., Zhang, H., Song, J., Zhang, R., Xu, R., Zhu, Q., Ma, S., Wang, P., Bi, X., et al. Deepseek-r1: Incentivizing reasoning capability in llms via reinforcement learning. *arXiv preprint arXiv:2501.12948*, 2025.
- Ho, J. and Ermon, S. Generative adversarial imitation learning. *Advances in neural information processing systems*, 29, 2016.
- Hu, E. J., Shen, Y., Wallis, P., Allen-Zhu, Z., Li, Y., Wang, S., Wang, L., and Chen, W. Lora: Low-rank adaptation of large language models. *arXiv preprint arXiv:2106.09685*, 2021.
- Huang, W., Abbeel, P., Pathak, D., and Mordatch, I. Language models as zero-shot planners: Extracting actionable knowledge for embodied agents. In *International conference on machine learning*, pp. 9118–9147. PMLR, 2022.
- Hussein, A., Gaber, M. M., Elyan, E., and Jayne, C. Imitation learning: A survey of learning methods. *ACM Computing Surveys (CSUR)*, 50(2):1–35, 2017.
- Jansen, P. A. Visually-grounded planning without vision: Language models infer detailed plans from high-level instructions. *arXiv preprint arXiv:2009.14259*, 2020.
- Jiao, F., Qin, C., Liu, Z., Chen, N. F., and Joty, S. Learning planning-based reasoning by trajectories collection and process reward synthesizing. *arXiv preprint arXiv:2402.00658*, 2024.
- Kocsis, L. and Szepesvári, C. Bandit based monte-carlo planning. In *European conference on machine learning*, pp. 282–293. Springer, 2006.
- Kolve, E., Mottaghi, R., Han, W., VanderBilt, E., Weihs, L., Herrasti, A., Deitke, M., Ehsani, K., Gordon, D., Zhu, Y., et al. Ai2-thor: An interactive 3d environment for visual ai. *arXiv preprint arXiv:1712.05474*, 2017.
- Li, C., Wong, C., Zhang, S., Usuyama, N., Liu, H., Yang, J., Naumann, T., Poon, H., and Gao, J. Llava-med: Training a large language-and-vision assistant for biomedicine in one day. *Advances in Neural Information Processing Systems*, 36, 2024.
- Li, J., Li, D., Savarese, S., and Hoi, S. Blip-2: Bootstrapping language-image pre-training with frozen image encoders and large language models. In *International conference on machine learning*, pp. 19730–19742. PMLR, 2023.
- Li, S., Puig, X., Paxton, C., Du, Y., Wang, C., Fan, L., Chen, T., Huang, D.-A., Akyürek, E., Anandkumar, A., et al. Pre-trained language models for interactive decision-making. *Advances in Neural Information Processing Systems*, 35:31199–31212, 2022.
- Liu, H., Li, C., Wu, Q., and Lee, Y. J. Visual instruction tuning. *Advances in neural information processing systems*, 36, 2024.
- Micheli, V. and Fleuret, F. Language models are few-shot butlers. *arXiv preprint arXiv:2104.07972*, 2021.

- Ng, A. Y. and Russell, S. J. Algorithms for inverse reinforcement learning. In *Proceedings of the 17th International Conference on Machine Learning (ICML)*, pp. 663–670, 2000.
- Rafailov, R., Sharma, A., Mitchell, E., Manning, C. D., Ermon, S., and Finn, C. Direct preference optimization: Your language model is secretly a reward model. *Advances in Neural Information Processing Systems*, 36, 2024.
- Rashidinejad, P., Zhu, B., Ma, C., Jiao, J., and Russell, S. Bridging offline reinforcement learning and imitation learning: A tale of pessimism. *Advances in Neural Information Processing Systems*, 34:11702–11716, 2021.
- Rosin, C. D. Multi-armed bandits with episode context. *Annals of Mathematics and Artificial Intelligence*, 61(3): 203–230, 2011.
- Ross, S. and Bagnell, D. Efficient reductions for imitation learning. In *Proceedings of the thirteenth international conference on artificial intelligence and statistics*, pp. 661–668. JMLR Workshop and Conference Proceedings, 2010.
- Ross, S., Gordon, G., and Bagnell, D. A reduction of imitation learning and structured prediction to no-regret online learning. In *Proceedings of the fourteenth international conference on artificial intelligence and statistics*, pp. 627–635. JMLR Workshop and Conference Proceedings, 2011.
- Schulman, J., Wolski, F., Dhariwal, P., Radford, A., and Klimov, O. Proximal policy optimization algorithms. *arXiv preprint arXiv:1707.06347*, 2017.
- Shinn, N., Cassano, F., Gopinath, A., Narasimhan, K., and Yao, S. Reflexion: Language agents with verbal reinforcement learning. *Advances in Neural Information Processing Systems*, 36, 2024.
- Shridhar, M., Thomason, J., Gordon, D., Bisk, Y., Han, W., Mottaghi, R., Zettlemoyer, L., and Fox, D. Alfred: A benchmark for interpreting grounded instructions for everyday tasks. In *Proceedings of the IEEE/CVF conference on computer vision and pattern recognition*, pp. 10740–10749, 2020a.
- Shridhar, M., Yuan, X., Côté, M.-A., Bisk, Y., Trischler, A., and Hausknecht, M. Alfworld: Aligning text and embodied environments for interactive learning. *arXiv preprint arXiv:2010.03768*, 2020b.
- Song, Y., Da Yin, X. Y., Huang, J., Li, S., and Lin, B. Y. Trial and error: Exploration-based trajectory optimization for llm agents, 2024. URL <https://arxiv.org/abs/2403.02502>.
- Song, Y., Yin, D., Yue, X., Huang, J., Li, S., and Lin, B. Y. Trial and error: Exploration-based trajectory optimization for llm agents. *arXiv preprint arXiv:2403.02502*, 2024.
- Stella, F., Della Santina, C., and Hughes, J. How can llms transform the robotic design process? *Nature machine intelligence*, 5(6):561–564, 2023.
- Team, G., Riviere, M., Pathak, S., Sessa, P. G., Hardin, C., Bhupatiraju, S., Hussenot, L., Mesnard, T., Shahriari, B., Ramé, A., et al. Gemma 2: Improving open language models at a practical size. *arXiv preprint arXiv:2408.00118*, 2024.
- Touvron, H., Lavril, T., Izacard, G., Martinet, X., Lachaux, M.-A., Lacroix, T., Rozière, B., Goyal, N., Hambro, E., Azhar, F., et al. Llama: Open and efficient foundation language models. *arXiv preprint arXiv:2302.13971*, 2023.
- Wang, H., Chin, N., Gonzalez-Pumariiega, G., Sun, X., Sunkara, N., Pace, M. A., Bohg, J., and Choudhury, S. Apricot: Active preference learning and constraint-aware task planning with llms. *arXiv preprint arXiv:2410.19656*, 2024a.
- Wang, P., Bai, S., Tan, S., Wang, S., Fan, Z., Bai, J., Chen, K., Liu, X., Wang, J., Ge, W., et al. Qwen2-vl: Enhancing vision-language model’s perception of the world at any resolution. *arXiv preprint arXiv:2409.12191*, 2024b.
- Wang, Z., Cai, S., Chen, G., Liu, A., Ma, X., and Liang, Y. Describe, explain, plan and select: Interactive planning with large language models enables open-world multi-task agents. *arXiv preprint arXiv:2302.01560*, 2023.
- Wei, J., Wang, X., Schuurmans, D., Bosma, M., Xia, F., Chi, E., Le, Q. V., Zhou, D., et al. Chain-of-thought prompting elicits reasoning in large language models. *Advances in neural information processing systems*, 35:24824–24837, 2022.
- Wu, J., Antonova, R., Kan, A., Lepert, M., Zeng, A., Song, S., Bohg, J., Rusinkiewicz, S., and Funkhouser, T. Tidybot: Personalized robot assistance with large language models. *Autonomous Robots*, 47(8):1087–1102, 2023a.
- Wu, Q., Bansal, G., Zhang, J., Wu, Y., Zhang, S., Zhu, E., Li, B., Jiang, L., Zhang, X., and Wang, C. Autogen: Enabling next-gen llm applications via multi-agent conversation framework. *arXiv preprint arXiv:2308.08155*, 2023b.
- Xie, Y., Goyal, A., Zheng, W., Kan, M.-Y., Lillicrap, T. P., Kawaguchi, K., and Shieh, M. Monte carlo tree search boosts reasoning via iterative preference learning. *arXiv preprint arXiv:2405.00451*, 2024.
- Xiong, W., Song, Y., Zhao, X., Wu, W., Wang, X., Wang, K., Li, C., Peng, W., and Li, S. Watch every step! llm

agent learning via iterative step-level process refinement. *arXiv preprint arXiv:2406.11176*, 2024.

Yang, Y., Zhou, T., Li, K., Tao, D., Li, L., Shen, L., He, X., Jiang, J., and Shi, Y. Embodied multi-modal agent trained by an llm from a parallel textworld. In *Proceedings of the IEEE/CVF Conference on Computer Vision and Pattern Recognition*, pp. 26275–26285, 2024.

Yao, S., Chen, H., Yang, J., and Narasimhan, K. Webshop: Towards scalable real-world web interaction with grounded language agents. *Advances in Neural Information Processing Systems*, 35:20744–20757, 2022a.

Yao, S., Zhao, J., Yu, D., Du, N., Shafran, I., Narasimhan, K., and Cao, Y. React: Synergizing reasoning and acting in language models. *arXiv preprint arXiv:2210.03629*, 2022b.

Yuan, Z., Yuan, H., Li, C., Dong, G., Lu, K., Tan, C., Zhou, C., and Zhou, J. Scaling relationship on learning mathematical reasoning with large language models. *arXiv preprint arXiv:2308.01825*, 2023.

Zelikman, E., Harik, G., Shao, Y., Jayasiri, V., Haber, N., and Goodman, N. D. Quiet-star: Language models can teach themselves to think before speaking. *arXiv preprint arXiv:2403.09629*, 2024.

Zhang, D., Zhou, S., Hu, Z., Yue, Y., Dong, Y., and Tang, J. Rest-mcts*: Llm self-training via process reward guided tree search. *arXiv preprint arXiv:2406.03816*, 2024.

Zhao, Z., Lee, W. S., and Hsu, D. Large language models as commonsense knowledge for large-scale task planning. *Advances in Neural Information Processing Systems*, 36, 2024.

Zhu, D., Chen, J., Shen, X., Li, X., and Elhoseiny, M. Minigt-4: Enhancing vision-language understanding with advanced large language models. *arXiv preprint arXiv:2304.10592*, 2023.

A. Proofs

A.1. Proof of Theorem 4.1

Each policy π_i is a mixed policy combining the expert policy π^* and learned policy $\hat{\pi}_i$ with a non-increasing mixing coefficient β_i , expressed as $\pi_i = \beta_i\pi^* + (1 - \beta_i)\hat{\pi}_i$, where the sequence $\hat{\pi}_{1:N}$ represents the policies $\hat{\pi}_1$ through $\hat{\pi}_N$. The term ϵ_N defines the loss of the best policy in hindsight after N iterations, calculated as $\min_{\pi \in \Pi} \frac{1}{N} \sum_{i=1}^N \mathbb{E}_{s \sim d_{\pi_i}} [\ell(s, \pi)]$. The variable ℓ_{max} serves as an upper bound on the loss, ensuring that $\ell_i(s, \hat{\pi}_i) \leq \ell_{max}$ holds for all policies $\hat{\pi}_i$ and states s where $d_{\hat{\pi}_i}(s) > 0$. The term n_β represents the largest value of n not exceeding N that satisfies $\beta_n > \frac{1}{T}$, while γ_N denotes the average regret observed across the policy sequence $\hat{\pi}_{1:N}$.

Lemma A.1. *For DAgger, there exists a policy $\hat{\pi} \in \hat{\pi}_{1:N}$ such that:*

$$\mathbb{E}_{s \sim d_{\hat{\pi}}} [\ell(s, \hat{\pi})] \leq \epsilon_N + \gamma_N + \frac{2\ell_{max}}{N} [n_\beta + T \sum_{i=n_\beta+1}^N \beta_i]$$

Based on Lemma A.1, we can prove that MCTS has better performance bounds than on-policy algorithms.

Proof. We begin by expressing the PUCT policy in terms of UCT and prior policy π_θ . Define policy model $\pi_{uct} = Q(s, a) + c \frac{\sqrt{\sum_b n(x, b)}}{1+n(x, a)}$, where for each step i , $Q(s_i, a)$ will update, so π_{uct} can be interpreted as iterative policy model π_{uct}^i with appropriate scaling.

The MCTS with PUCT policy can be written as:

$$\pi_{mcts}^i = \pi_{uct}^i + c * \frac{\sqrt{\sum_b n(x, b)}}{1+n(x, a)} (\pi_\theta - 1).$$

Let $c_i = c \frac{\sqrt{\sum_b n(x, b)}}{1+n(x, a)}$, we can rewrite π_{mcts} as:

$$\pi_{mcts}^i \propto \frac{1}{c_i + 1} \pi_{uct}^i + \frac{c_i}{1 + c_i} (\pi_\theta - 1) = (1 - \beta_i) \pi_{uct}^i + \beta_i (\pi_\theta - 1)$$

where $\beta_i = \frac{c_i}{1+c_i}$. Note that the \propto holds because we use argmax for action selection in π_{mcts} , and scaling by a constant $(1 + c_i)$ does not affect the argmax operation.

The proof relies on three key conditions:

1. UCT Regret Bound: From (Auer, 2002), the cumulative regret $R(T)$ of UCT grows as $O(\ln n)$ in specific cases, it is a no-regret algorithm:

$$\lim_{T \rightarrow \infty} \frac{R(T)}{T} = 0$$

2. Decay of Mixing Coefficient: As $N \rightarrow \infty$, $\frac{c_i}{1+c_i}$ decreases to a positive constant. To ensure $\overline{\beta_N} = \frac{1}{N} \sum_{i=1}^N \beta_i \rightarrow 0$ as $N \rightarrow \infty$, we can simple set $\beta_i = I(i = 1)$.

3. Loss Function Property: The loss function is strongly convex.

Let $\epsilon_N = \min_{\pi \in \Pi} \frac{1}{N} \sum_{i=1}^N \mathbb{E}_{s \sim d_{\pi_{mcts}^i}} [l(s, \pi)]$ represent the loss of the best policy. From Lemma A.1, there exists a policy π_{uct}^i such that:

$$\mathbb{E}_{s \sim d_{\pi_{uct}^i}} (l(s, \pi_{uct}^i)) \leq \epsilon_N + \gamma_N + \frac{2\ell_{max}}{N} [n_\beta + T \sum_{i=n_\beta+1}^N \beta_i], \quad (10)$$

where γ_N is the average regret of π_{uct}^0 to π_{uct}^N . As $N \rightarrow \infty$, π_{uct} is no-regret, then $\gamma_N \rightarrow 0$ and the last term approaches 0.

Since ϵ_N represents the loss of the optimal policy, we have $\epsilon_N \leq \mathbb{E}_{s \sim d_{\pi_{mcts}^i}} [l(s, \pi_\theta)]$. Furthermore, given that the loss function $l(s, \cdot)$ is convex in π for all states s , we can derive:

$$\mathbb{E}_{s \sim d_{\pi_{mcts}^i}} [l(s, \pi_{mcts}^i)] \leq (1 - \beta_i) \mathbb{E}_{s \sim d_{\hat{\pi}_i}} [l(s, \hat{\pi}_i)] + \beta_i \mathbb{E}_{s \sim d_{\pi_{mcts}^i}} [l(s, \pi_\theta)] \leq \mathbb{E}_{s \sim d_{\pi_{mcts}^i}} [l(s, \pi_\theta)] \quad (11)$$

□

A.2. Proof of Theorem 4.2

Proof. Inverse reinforcement learning (IRL) (Ng & Russell, 2000) primitive procedure can be defined as

$$IRL_{\psi}(\pi_E) = \operatorname{argmax}_{c \in \mathbb{R}^{S \times A}} -\psi(c) + \left(\min_{\pi \in \Pi} -H(\pi) + \mathbb{E}_{\pi}[c(s, a)] \right) - \mathbb{E}_{\pi_E}[c(s, a)] \quad (12)$$

where ψ is cost regularization, c is the cost function, $H(\pi) = \mathbb{E}_{\pi}[-\log \pi(a|s)]$, π is learned policy and π_E is expert policy. It is a max-min problem. IRL can generate optimal cost function. Define $RL(c)$ to generate optimal policy:

$$RL(c) = \operatorname{argmin}_{\pi \in \Pi} -H(\pi) + \mathbb{E}_{\pi}[c(s, a)] \quad (13)$$

If $\tilde{c} \in \text{IRL}_{\psi}(\pi_E)$, we want to get optimal policy by $RL(\tilde{c})$. Then the dual problem of equation 12 with some relax is :

$$\text{RL} \circ \text{IRL}_{\psi}(\pi_E) = \operatorname{argmin}_{\pi \in \Pi} -H(\pi) + \psi^*(\rho_{\pi} - \rho_{\pi_E}). \quad (14)$$

where $\rho_{\pi}(s, a) = \pi(a|s) \sum_{t=0}^{\infty} \gamma^t P(s_t = s | \pi)$ can be interpreted as the distribution of state-action pairs that an agent encounters when navigating the environment with policy π , ψ^* is the dual function of cost regularization ψ .

The proof consists of three key steps:

1) First, we establish that $\psi(a)$ is a valid convex regularization function on $S \times A \rightarrow \mathbb{R}$. Its convex conjugate is:

$$\psi^*(\rho_{\pi} - \rho_{\pi_E}) = \sup_a \{(\rho_{\pi} - \rho_{\pi_E})^T a - \psi(a)\} \quad (15)$$

$$= -\mathbb{E}_{\pi_E}[\log \pi_E(a|s)] + \sup_a \{(\rho_{\pi} - \rho_{\pi_E})^T a - c * \frac{\sqrt{ln t}}{t * \rho_{\pi}(s, a)}\}. \quad (16)$$

2) The occupancy measure $\rho_{\pi}(s, a) = \pi(a|s) \sum_t \gamma^t P(s_t = s | \pi)$ represents the discounted visitation frequency of state-action pairs under policy π . In the MCTS context, $t * \rho_{\pi}(s, a)$ is proportional to the visit count $N(s, a)$, as both measure the frequency of state-action selections.

3) The second term in equation 15 corresponds to the Lower Confidence Bound (LCB) formulation approximately (Rashidinejad et al., 2021). By defining π_E as the policy derived from preferred actions and π as the policy over rejected actions, we obtain:

$$\begin{aligned} \text{RL} \circ \text{IRL}_{\psi}(\pi_E) = & \operatorname{argmin}_{\pi \in \Pi} -\mathbb{E}_{\pi_E}[\log \pi_E(a|s)] + \mathbb{E}_{\pi}[\log \pi(a|s)] \\ & + \sup_a \{(\rho_{\pi} - \rho_{\pi_E})^T a - c * \frac{\sqrt{ln t}}{t * \rho_{\pi}(s, a)}\} \end{aligned} \quad (17)$$

This formulation reveals a two-stage optimization process:

- Stage 1 (IRL): The LCB policy generates a value function serving as the cost function in IRL
- Stage 2 (RL): DPO maximizes the log-probability difference between preferred and rejected actions

This completes the connection between MCTS-EP and the GAIL framework. □

B. Experiment Settings

B.1. Dataset Details

ALFWorld tasks involve natural language goal descriptions (e.g., “put a pan on the dining table”) and require agents to perform high-level actions such as go to, clean and opening. The framework includes six task types: Pick & Place, Clean &

Place, Heat & Place, Cool & Place, Look in Light, and Pick Two Objects & Place. These tasks challenge agents to navigate visually diverse environments, interact with up to 120 dynamically populated rooms, and manipulate portable objects (e.g., apples, mugs) and static receptacles (e.g., drawers, microwaves). To enable cross-modal learning, ALFWorld uses the TextWorld engine (Côté et al., 2019) to generate text-based analogs of ALFRED scenes, described using the Planning Domain Definition Language (PDDL) (Aeronautiques et al., 1998). Each scene’s state and dynamics are mirrored across modalities, allowing agents to train and evaluate in either the visual or text-based environment.

B.2. Hyperparameters Details

For single-modal training, we apply LoRA (Hu et al., 2021) fine-tuning on Llama-3.1-8B-Instruct with a sequence length of 2048, a device batch size of 1, and a learning rate of $5e-5$ using a cosine scheduler, fine-tuning for 2 epochs with 8 gradient accumulation steps. For multi-modal tasks, we use Qwen2-VL-7B-Instruct, unfreezing the vision tower during fine-tuning with a learning rate of $1e-4$ and a batch size of 4 per device. For multi-modal DPO, only the backbone is fine-tuned, with the learning rate reduced to $5e-6$ for stability. Across all experiments, we set the LoRA rank to 16 and use a sigmoid preference loss function with β set to 0.5.

B.3. System Prompts

Text-Only Prompt

You are an AI robot agent in an interactive environment. Your goal is to accomplish the given task through a series of actions. Follow these guidelines:

- Carefully analyze the task requirements. Break down complex tasks into smaller, manageable steps and create a mental plan before acting
- Be persistent in searching for required objects. When searching for objects, use common sense to predict likely locations, then systematically explore those areas
- For tasks involving multiple objects, keep a mental count of how many you’ve collected or placed
- Avoid repeating the same action consecutively. If an action doesn’t work, explore other objects or locations
- Your response must be exactly one action name chosen strictly from provided candidate actions

Figure 2. Text-Only Prompt

Multi-Modal Prompt

You are an AI robot agent in an interactive environment. Your goal is to accomplish the given task through a series of actions. Follow these guidelines:

- Carefully analyze the task requirements. When searching for objects, use common sense to predict likely locations
- For tasks involving multiple objects, keep a mental count of collected or placed items
- Respond only with a JSON object containing:
 - **"what_you_see"**: your detailed observation
 - **"action"**: one action name

Figure 3. Multi-Modal Prompt